VOL. 10, NO. 23, DECEMBER 2015 ISSN 1819-6608
ARPN Journal of Engineering and Applied Sciences

www.arpnjournals.com

DEVELOPMENT AND CONTROL OF A 3DOF UPPER-LIMB ROBOTIC DEVICE FOR PATIENTS WITH PARETIC LIMB IMPAIRMENT

Sado Fatai, Shahrul N. Sidek, Yusof M. Hazlina, Latif M. Hafiz and Adamu Y. Babawuro
Department of Mechatronics Engineering, International Islamic University Malaysia, Malaysia
E-Mail: abdfsado1@gmail.com

ABSTRACT

Rehabilitation therapy after stroke is crucial to helping patients regain as much as possible the use of their paretic limbs. The major challenges, however, in conventional post-stroke rehabilitation therapy is that the therapy is labour-intensive, time demanding, and therefore, expensive with consequent reduction in the amount of training session required for optimal therapeutic outcome. In recent times, the use of robotic devices for rehabilitation training has been widely favoured. Robot-assisted rehabilitation therapy is cost-effective, fatigue-free, and has the potential to improve the efficiency of the rehabilitation process. More so, positive outcome of improved motor control abilities for patients undergoing robot-assisted therapy have been widely recorded. This paper presents the development and control of a portable three degree of freedom (3-DOF) end-effector-type robotic device for upper-extremity rehabilitation of paretic stroke patients. The device has three active DOFs consisting of two revolute joints and one prismatic joint (R-R-P) designed to allow 3-dimensional range of motion (ROM) exercise for elbow and shoulder rehabilitation. A novel adaptive hybrid impedance control framework has been developed for the device to allow safe robot-patient dynamic interaction during planned repetitive range of motion exercises and to keep track of patients' motor recovery based on an embedded Modified Ashworth Scale assessment criteria. Experimental results performed, using a healthy subject, to test and evaluate the ability of the device to track a planned simple flexion/extension range of motion exercise for the elbow joint showed position and force tracking accuracy to a maximum root mean square error (RMSE) of 0.024m and 0.343N respectively which indicate the possibility of use of the device for real patients.

Keywords: upper-extremity, robot-assisted, rehabilitation, hybrid impedance.

INTRODUCTION

In the last few decades, the increasing cases of upper-extremity disabilities resulting from stroke, spinal cord injuries (SCI), and other related illness have favoured the use of robotic devices to provide assistance and support to patients undergoing rehabilitation therapy[1, 2]. The effectiveness of the devices in extending the therapy session and in providing repetitive exercises aimed at inducing motor plasticity have been widely reported [2, 3]. Robotic devices have the potentials of allowing repeatability and automation of therapeutic procedures with significant improvement on the efficiency of the rehabilitation process [4]. With the increasing demand, however, for robotic devices, the need for portable, lightweight, and safe devices have created new challenges ranging from the design of compact robot mechanical/actuation systems to the development of effective control algorithms.

A survey on robotic devices in the recent past, showed that most of the earlier robotic devices and some of the recent commercially available ones are mechanically bulky and suited for use only in rehabilitation centres [5-7]. Besides, most are less autonomous to the extent that they require constant assistance of a human therapist for effective usage, for task specification and for adjustment of therapy [7]. This implies a considerable amount of valuable therapist time in programming the robot, monitoring the patients, analysing data from the robot and also assessing the progress of the patients

Krebs *et al.*[8] and Lum *et al.*[9] earlier proposed a 3-DOF robotic device that allowed horizontal motion and a 6-DOF Mirror Image Movement Enabler (MIME) robotic device that allowed 3-dimensional spatial motion, respectively, for upper-limb rehabilitation which were generally bulky and suited only for rehabilitation centres. The devices were less autonomous and require the manual monitoring of patients' progress by an expert therapist. A 9-DOF cable-driven robotic device was also proposed by [10] based on GENTLE/S system. The device was effectively used for reach and grasp therapy for post-stroke patients, but was equally bulky and non-adaptive to patients' recovery. A more recent commercially available robotic device referred to as ArmeoPower [11] with 7-DOF for elbow and shoulder rehabilitation and additional DOFs for wrist and fingers flexion/extension rehabilitation exercise which has been successfully used in many rehabilitation centres is also seen to be largely stationary and not lightweight. As development of robotic devices for rehabilitation exercises continue, the need for portable and lightweight devices capable of autonomous guidance and monitoring of patients' progress therefore remains a critical driving factor of consideration [7].

In this study, we report the development and control of a 3-DOF end-effector robotic device for autonomous rehabilitation of the shoulder and elbow region of patients with paretic upper-limb impairment. The device is made portable and lightweight to allow flexibility of usage and for possible use at homes. In addition, a novel adaptive control framework reported in [12] is developed for the device to allow safe robot-

patients dynamic interaction and effective tracking of a planned range of motion exercise, and independent monitoring of patients' physical recovery progress.

The rest of the paper is organized as follows: section 2 reports on the kinematics and dynamic modelling of the robotic device, section 3 presents the features of the developed novel robot control framework, section 4 presents some experimental results and discussion and section 5 concludes the paper with proposed future works.

ROBOT MODELING

Forward kinematics

The robotic device has three active DOF arranged in a revolute-revolute-prismatic (R-R-P) configuration with only two link lengths, l_2 and l_(3) parameters (to simplify the inverse kinematics) as shown in Figure-1 and Figure-2. The three joints allow for the rehabilitation (flexion, extension, abduction, and adduction) of the elbow and shoulder of the patients in three dimensional space. The relationship between the joints variables and the position and orientation of the robot's end-effector is derived from the four Denavit-Hartenberg (DH) parameters given in Table-1. The four parameters a_i,∝_i, d_i, θ_i are generally known as the link length, link twist, link offset, and joint angles respectively[13].

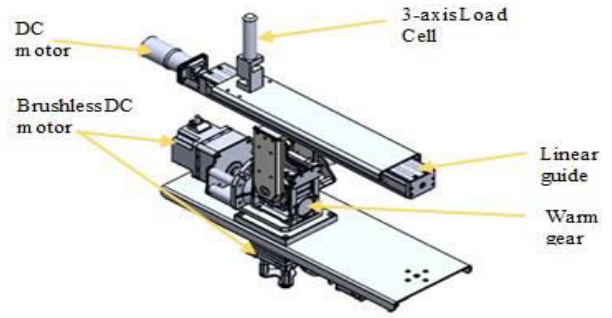

Figure-1. The Mechanical structure of the 3-DOF robotic device.

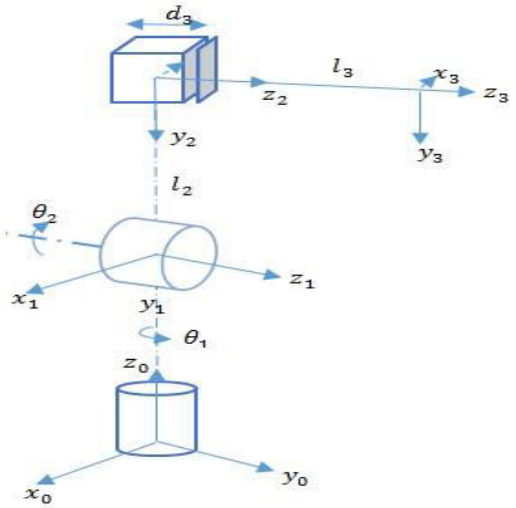

Figure-2. The robot kinematic model.

The link transformation matrices which relates any two successive frames attached to the joints are derived from the homogenous transformation matrice [13] given by Equation (1).

$$ {}^{i-1}_{i}T = \begin{bmatrix} c\theta_i & -s\theta_i & 0 & a_{i-1} \\ s\theta_i c\alpha_{i-1} & c\theta_i c\alpha_{i-1} & -s\alpha_{i-1} & -s\alpha_{i-1}d_i \\ s\theta_i s\alpha_{i-1} & c\theta_i s\alpha_{i-1} & c\alpha_{i-1} & c\alpha_{i-1}d_i \\ 0 & 0 & 0 & 1 \end{bmatrix} \quad (1) $$

where s and c stands for sine and cosine of the angles. The homogenous transformation matrix relating the end-effector frame (x_3, y_3, z_3) to the base frame (x_0, y_0, z_0), see Figure-2, is therefore obtained by multiplying the individual link transformation matrices as shown in Equation (2).

$$ {}^{0}_{3}T = {}^{0}_{1}T \; x \; {}^{1}_{2}T \; x \; {}^{2}_{3}T \quad (2) $$

Finally, the forward kinematics equation derived from Equation (2) is expressed as,

$$ \begin{bmatrix} x \\ y \\ z \end{bmatrix} = \begin{bmatrix} c\theta_1(lc\theta_2 + d_3 s\theta_2) \\ s\theta_1(lc\theta_2 + d_3 s\theta_2) \\ d_3 c\theta_2 - ls\theta_2 \end{bmatrix} \quad (3) $$

Table-1. The DH-parameters.

Link	a_i	α_i	d_i	θ_i
1	0	-90	0	θ_1^*
2	*l*	90	*0*	θ_2^*
3	*0*	0	d_3^*	0

Inverse kinematics

We derive the inverse kinematics of the rehabilitation robot in order to determine the joint angles or variables in terms of the end-effector position and orientation. It is however more computationally demanding than the forward kinematics analysis due to the non-linearity in the forward kinematics equation. Since the robotic device is designed with two axis intersecting, the inverse kinematic analysis becomes fairly easy with a possible closed form solution.

Observing that the forward kinematics equations are transcendental, the following substitutions are made

$$ u_i = \tan\frac{\theta_i}{2}, \cos\theta_i = \frac{1-u_i^2}{1+u_i^2}, \; \sin\theta_i = \frac{2u_i}{1+u_i^2} \quad (4) $$

where u_i denotes the tangent of any half angle, and $i = 1,2$. By substituting Equation (4) in Equation (3) and solving for the joint variables $q = [\theta_1 \quad \theta_2 \quad d_3]$, we obtain the inverse kinematics equations for the robotic system as

$$\left.\begin{aligned}\theta_1 &= \text{Atan } 2(\pm\tfrac{y}{x}, 1)\\ \theta_2 &= \text{Atan2}(-l \pm \sqrt{l^2 + (\tfrac{d_3 - z}{d_3 + z})}, 1)\\ d_3 &= \pm\sqrt{x^2 + y^2 + z^2 - l^2}\end{aligned}\right\} \quad (5)$$

The solution is however not unique since there is the possibility of different configurations (some unreachable) for a given solution. We therefore avoids the use of the inverse kinematics for the controller development as will be seen in the next section.

Velocity kinematics: The Jacobian

The velocity kinematics equation relates the linear velocity v and angular velocity q˙ of the end-effector to the joint velocities of the robotic device. Similar to the forward kinematics equation, it defines a function which maps between the Cartesian space and joint space. This relationship is expressed by the Jacobian time-varying linear transformation given by Equation (6).

$$v = J(q)\,\dot{q} \quad (6)$$

Taking the first derivative of the forward kinematics equations (refer to Equation (3)) and using the techniques described in [13], we obtain the Jacobian given as

$$J = \begin{bmatrix} -s_1(lc_2 + d_3 s_2) & -c_1(lc_2 + d_3 s_2) & c_1 s_2 \\ c_1(lc_2 + d_3 s_2) & -s_1(lc_2 + d_3 s_2) & s_1 s_2 \\ 0 & k & c_2 \\ 0 & -s_1 & 0 \\ 0 & -c_1 & 0 \\ 1 & 0 & 0 \end{bmatrix} \quad (7)$$

Where,

$$k = -{c_1}^2(lc_2 + d_3 s_2) - {s_1}^2(lc_2 + d_3 s_2)$$

The robot dynamics

To obtain the robot dynamic model, we use the Lagrange equation of motion [14] for a conservative system given by

$$\frac{d}{dt}\frac{\partial L}{\partial \dot{q}} - \frac{\partial L}{\partial q} = \tau \quad (8)$$

where q is the 3x1 vector of generalized joint coordinates, τ is the 3x1 vector of generalized input actuator forces/torque, and L the Lagrangian.
The Lagrangian is given by the expression,

$$L = K - P \quad (9)$$

where K is the kinematic energy of the robotic system, and P is the potential energy of the system. Using Equation (8)-(9), we derive the overall dynamic model of the robotic device expressed by Equation (10) which is a requisite for developing the control algorithm.

$$M_r(q)\ddot{q} + I_{act}\ddot{q} + C(q,\dot{q})\dot{q} + G(q) = \tau \quad (10)$$

M_r represents the robot mass matrix, I_{act} represents the actuator inertia, $C(q,\dot{q})$ represents the Coriolis and centrifugal terms, and $G(q)$ represents the gravity term. Since the joint frictions are small for the robotic device, we assumed these components to be zero in the robot dynamic model.

CONTROL ARCHITECTURE

Sensors and actuation system

A DC motor coupled at the prismatic joint, at frame (x_2, y_2, z_2), provide linear actuation by means of a lead screw mechanism to allow flexion and extension of the elbow joint along 90° to the supine (other configurations are possible when actuation is done in conjunction with other joints actuation), see Figure-1 and Figure-2. The DC motor is equipped with incremental encoder which gives precise measurement of linear position, velocity and acceleration of the end-effector. The other two revolute joints at frame (x_0, y_0, z_0): denoted base frame, and frame (x_1, y_1, z_1) are actuated separately by means of brushless DC motors with coupled incremental encoders to allow precise measurement of joint angular positions, velocities, and accelerations along their respective frames. Actuation of the base frame allows for rotational motion along the vertical axis (z_0) which assist shoulder reshabilitation, and in conjunction with the second joint actuation allows abduction and adduction ROM exercises of the shoulder. The actuation of the second joint at frame (x_1, y_1, z_1) allows tilting or rotational motion along the horizontal axis (z_1). In addition, contact force measurement is achieved at the end-effector location by means of a 3-axis load cell custom fabricated into the end-effector (see Figure-1).

Control hardware

A hardware control unit designed for the robotic device consists of a central microcontroller (Arduino Mega), see Figure-3. The microcontroller provides interface between the Matlab/Simulink control model on the PC side and the robotic device. The unit also consists of motor drivers which provide interface between the microcontroller and the motors, including the PWM to analog voltage converters which outputs analog voltage corresponding to the control torque on the PC side for tuning of the motor speed.

Figure-3. Control hardware.

Feedback control linearization strategy

Since the robot interacts with an environment (patients or human subjects in this case) with 3x1 joint space reaction torques given by τ_e, the robot-patient dynamic motion given by Equation (10) is modified as

$$M(q)\ddot{q} + I_{act}\ddot{q} + C(q,\dot{q})\dot{q} + G(q) = \tau - \tau_e \quad (11)$$

The vector of environment reaction torque τ_e in joint space is related to the task space contact force f_e by the Jacobian matrix $J(q)$ given by

$$\tau_e = J^T(q) f_e \quad (12)$$

Equation (11) can thus be rewritten as

$$\tau = M(q)\ddot{q} + C(q,\dot{q})\dot{q} + G(q) + J^T(q) f_e \quad (13)$$

where $M(q)$ represents the sum of the total robot mass matrix and the actuators inertia ($M_r(q) + I_{act}$).

We achieved the control objective by linearizing the non-linear dynamic equation given by Equation (13) using the concept of inner/outer loop control strategy [15] as shown in Figure-4. The inner loop represents the non-linear feedback linearization or inverse dynamics control (given by Equation 14) and the outer-loop represent a hybrid impedance control strategies (given by Equation 15).

$$\tau = M(q)J^{-1}(q)(\boldsymbol{a} - J(q)\dot{q}) + N(q,\dot{q}) + J^T(q) f_e \quad (14)$$

$$\boldsymbol{a} = SM_m{}^{-1}\left((f_e - f_d) - B_m\dot{x}\right) + (I - S)(\ddot{x}_d + \frac{B_m}{M_m}(\dot{x}_d - \dot{x}) + \frac{K_m}{M_m}(x_d - x) - \frac{1}{M_m} f_e) \quad (15)$$

where M_m, B_m, and K_m represent the robot virtual impedance parameters (mass, damping and stiffness factors), S represents the selector matrix for force and position control, f_d represents the reference force, and x_d represents the reference position.

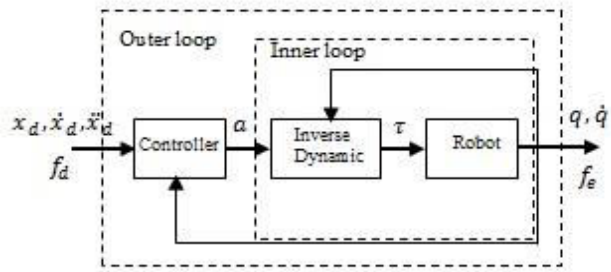

Figure-4. Inner and outer loop control strategy.

Adaptive control

We developed an adaptive control framework (to allow task space switching of position and force control as well as monitoring of patients' physical recovery progress) using a novel hybrid automata (HA) framework and an autoregressive exogenous recursive polynomial model estimator (ARX-RPME) as reported in earlier works [12], see Figure-5 for the adaptive framework. The RPME implements an ARX model of the upper-limb to estimate the mechanical impedance parameters of the limb as a measure of muscle tone. The estimated parameters serve as the inputs to the HA framework by means of which the automata accomplish two tasks. First, allows transition between its seven-state ($S_0 \ldots S_6$) automaton (including a default transition state) based on the level of muscle tone (impairment) as classified by the Modified Ashworth Scale (MAS) assessment criteria [12, 16], and second, allows switching, concurrently, of task space between force and position control, based on the changing upper-limb mechanical impedance and the interpretation of the duality principle[17, 18]. Figure-6 gives the overall control framework.

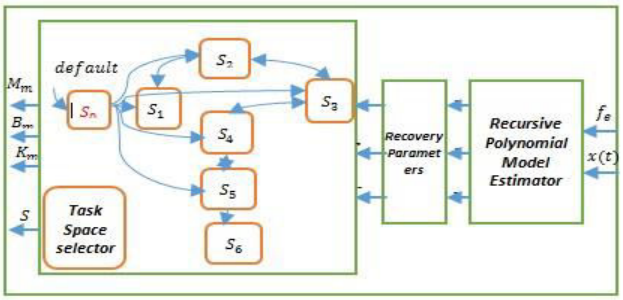

Figure-5. The ARX-RPME and the HA model.

RESULTS

As a preliminary experimentation on the device, we tested its ability to follow a planned reference ROM trajectory of the end-effector, and also on its ability to maintain a certain reference interactive force at the end-effector/human contact point.

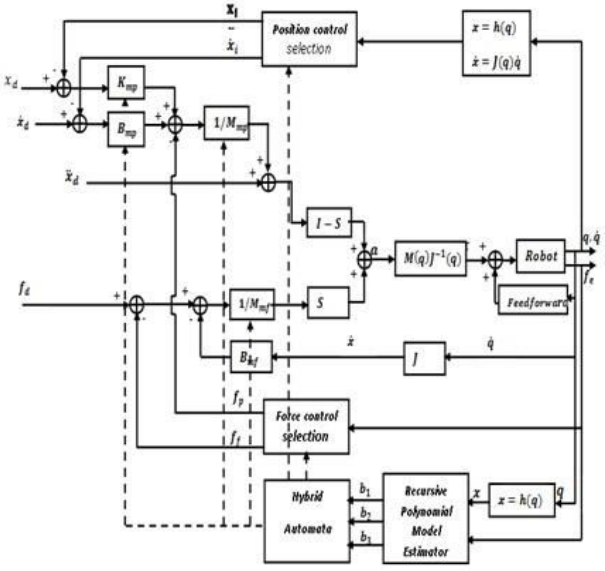

Figure-6. The overall adaptive control framework.

Trajectory generation and position control

To actualize the position control, we recorded (using a healthy subject) a simple elbow flexion range of motion exercise of the end-effector along the positive x, y, z direction and derive the reference trajectory (from the data) using a second order polynomial (see Equation 16). Figure-7 shows the position tracking results for the actual and desired position trajectory of the end-effector along the x,y,z directions with RMSE of 0.023, 0.024, and 0.013m respectively.

$$\begin{bmatrix} x_d(t) \\ y_d(t) \\ z_d(t) \end{bmatrix} = \begin{bmatrix} -0.0005t^2 - 0.0009t + 0.1521 \\ 0.0004t^2 - 0.0164t + 0.0078 \\ 0.0000t^2 - 0.0144t + 0.0012 \end{bmatrix} \quad (16)$$

Force tracking

To test the robotic device/controller on the ability to maintain certain amount of contact force (exerted by the end-effector on the environment/subject's limb), we planned a reference force trajectory using a 4th order polynomial such that the robot end-effector is made to exert force (by actuating the individual joints) on the subject's upper-limb steadily from zero to a maximum of 50N, and thereafter reduce the exerted force gradually to zero over a computer time of 21s. The generated reference trajectory along the positive z-direction of the end-effector is given by Equation (17). Figure-8 shows the force tracking results by the controller along the z-direction with RMSE of 0.343N.

$$f_{dz}(t) = 0.0009t^4 - 0.0347t^3 + 0.3535t^2 - 0.517t - 0.7265 \quad (17)$$

Discussion

As can be seen from the Figure-8, there is fairly good tracking of the reference force trajectory due to noise from the custom-made force sensor. As a modification, for future studies, a signal conditioning circuit will be adopted therefore to eliminate noisy signals. Regarding stability, no analysis for controller stability is given in this paper since the stability of control frameworks based on the standard computed torque control, or inverse dynamic control, have been generally established. However, mechanical stability is guaranteed using worm gears and a firm tripod support.

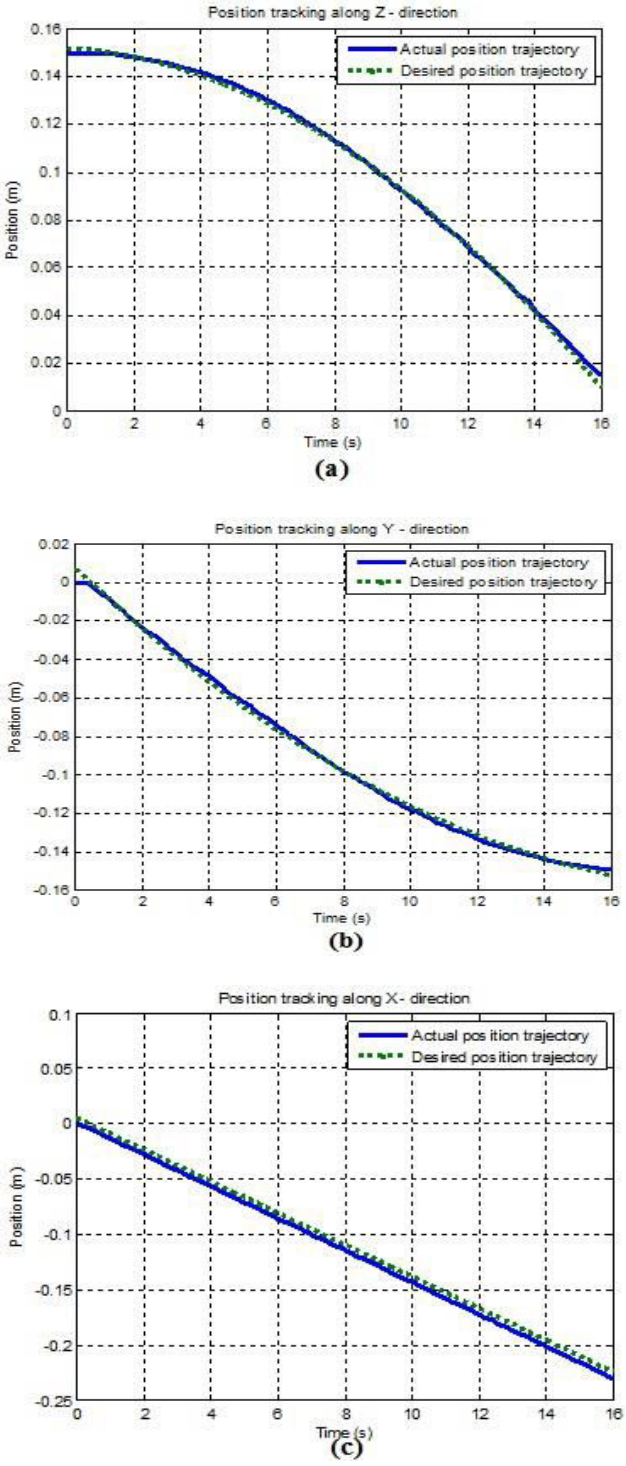

Figure-7. Experimental results for position tracking in the (a) z-direction (b) y-direction and (z) x-direction.

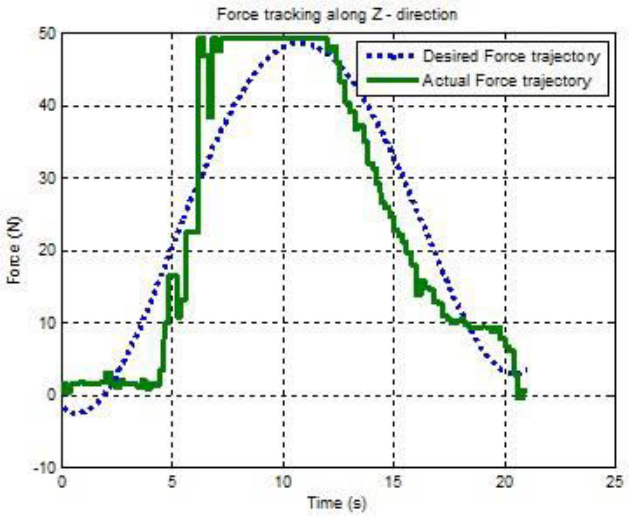

Figure-8. Experimental results for force tracking along the z-direction.

CONCLUSIONS

A new portable 3-DOF end-effector robotic device for autonomous rehabilitation of the shoulder and elbow region of patients with paretic upper-limb impairment has been presented. A novel adaptive control framework developed in previous study, by the Author, is adopted to allow safe robot-patients dynamic interaction and effective tracking of a planned range of motion exercise, as well as independent monitoring of patients' physical recovery progress.

Experimental results have shown the feasibility of use of the device for trajectory motion tracking of a reference ROM exercise. Future works however includes experimentation to test the adaptability of the robot control scheme to changing upper-limb mechanical impedance and final experimentation on actual patients.

REFERENCES

[1] M. J. O'Donnell, D. Xavier, L. Liu, H. Zhang, S. L. Chin and P. Rao-Melacini *et al.* 2010. "Risk factors for ischaemic and intracerebral haemorrhagic stroke in 22 countries (the INTERSTROKE study): a case-control study," The Lancet, Vol. 376, pp. 112-123.

[2] P. Maciejasz, J. Eschweiler, K. Gerlach-Hahn, A. Jansen-Troy, and S. Leonhardt. 2014. "A survey on robotic devices for upper limb rehabilitation," Journal of neuroengineering and rehabilitation, Vol. 11.

[3] H. S. Lo and S. Q. Xie. 2012. "Exoskeleton robots for upper-limb rehabilitation: state of the art and future prospects," Medical engineering & physics, Vol. 34, pp. 261-268.

[4] T. Nef, M. Mihelj and R. Riener. 2007. "ARMin: a robot for patient-cooperative arm therapy," Medical & biological engineering & computing, Vol. 45, pp. 887-900.

[5] R. Bogue. 2009. "Exoskeletons and robotic prosthetics: a review of recent developments," Industrial Robot: An International Journal, Vol. 36, pp. 421-427, 2009.

[6] B. Dellon and Y. Matsuoka. 2007. "Prosthetics, exoskeletons, and rehabilitation," IEEE Robotics and Automation magazine, Vol. 14, p. 30.

[7] I. Díaz, J. J. Gil and E. Sánchez. 2011. "Lower-limb robotic rehabilitation: literature review and challenges," Journal of Robotics, Vol. 2011.

[8] H. I. Krebs, M. Ferraro, S. P. Buerger, M. J. Newbery, A. Makiyama, M. Sandmann. *et al.* 2004. "Rehabilitation robotics: pilot trial of a spatial extension for MIT-Manus," Journal of NeuroEngineering and Rehabilitation, Vol. 1, pp. 5, 2004.

[9] P. S. Lum, C. G. Burgar, M. Van der Loos, P. C. Shor, M. Majmundar and R. Yap. 2006. "MIME robotic device for upper-limb neurorehabilitation in subacute stroke subjects: A follow-up study," Journal of rehabilitation research and development, Vol. 43, p. 631.

[10] R. C. Loureiro and W. S. Harwin. 2007. "Reach & grasp therapy: design and control of a 9-DOF robotic neuro-rehabilitation system," in Rehabilitation Robotics, 2007. ICORR 2007. IEEE 10th International Conference on, pp. 757-763.

[11] T. Nef, M. Guidali, V. Klamroth-Marganska and R. Riener. 2009. "ARMin-exoskeleton robot for stroke rehabilitation," in World Congress on Medical Physics and Biomedical Engineering, September 7-12, 2009, Munich, Germany, pp. 127-130.

[12] F. Sado, S. N. Sidek and H. M. Yusof. 2014. "Adaptive hybrid impedance control for a 3DOF upper limb rehabilitation robot using hybrid automata," in Biomedical Engineering and Sciences (IECBES), 2014 IEEE Conference on, pp. 596-601.

[13] M. W. Spong, S. Hutchinson and M. Vidyasagar. 2006. Robot modeling and control: John Wiley & Sons New York.

[14] S. B. Niku. 2001. Introduction to robotics: analysis, systems, applications Vol. 7: Prentice Hall New Jersey.

[15] R. Anderson and M. W. Spong. 1988. "Hybrid impedance control of robotic manipulators," Robotics and Automation, IEEE Journal of, vol. 4, pp. 549-556.

[16] R. W. Bohannon and M. B. Smith. 1987. "Interrater reliability of a modified Ashworth scale of muscle spasticity," Physical therapy, Vol. 67, pp. 206-207.

[17] F. L. Lewis D. M. Dawson and C. T. Abdallah. 2003. Robot manipulator control: theory and practice: CRC Press.

[18] M. W. Spong, S. Hutchinson and M. Vidyasagar. 2006. Robot modeling and control: John Wiley & Sons New York.